Abrasion Resistance of Sputtered Hard Coatings

P. Berghofer, Materials Center Leoben, Department of Physical Metallurgy and Materials Testing, University of Leoben (Austria); G. Tischler, P.H. Mayrhofer, C. Mitterer, Department of Physical Metallurgy and Materials Testing, University of Leoben (Austria)

Introduction

Numerous applications where surface engineering has been applied successfully like cutting or forming processes require enhanced wear resistance (1). Out of the main wear mechanisms identified to determine lifetime of tools, a considerable amount of abrasive wear takes place when particles, which are harder than the tool material, are involved. These particles can typically be carbides or oxides (e.g. when cutting steel) or highly strain-hardened fragments (e.g. wear debris generated during deep-drawing). Typically, abrasion resistance is evaluated using wear tests where the bulk mass loss or dimensional changes are monitored (2). However, for the characterisation of the abrasion resistance of surface engineered tool materials on a laboratory scale, a test method where very small samples can be used is highly attractive (3).

The aim of this paper is to evaluate the abrasion resistance of hard coatings deposited by Physical Vapour Deposition (PVD) onto steel substrates. In pursuit of this programme, sputtered CrN_x and superhard Ti-B-C coatings have been tested using a micro-abrasion test.

Experimental Details

All coatings investigated have been deposited using an unbalanced magnetron sputtering plant described in detail earlier (4). Cr-N coatings were grown by reactive sputtering in Ar/N_2 atmospheres using a Cr target (5). Different N/Cr atomic ratios as characterized by wavelength-dispersive electron probe microanalysis have been adjusted by the N_2 flow rate resulting in the phase compositions (characterized by X-ray diffraction (5)) given in Table 1. In addition, a nanocomposite Ti-B-C coating composed of TiB_2 and TiC has been deposited non-reactively using the same unbalanced magnetron sputtering unit by co-sputtering from TiB_2 and TiC targets (6) (see Table 1). As substrates, ground and polished austenitic stainless steel (DIN 1.4301, hardness 200 HV) samples with dimensions Ø 25 _ 4 mm and 20 _ 20 _ 1 mm were used.

Coating	Chemical composition	Phase composition	Hardness (GPa)	Thickness (µm)
Cr-N 1	Cr	Cr	8.5	5.7
Cr-N 2	$CrN_{0.19}$	$Cr(N) + Cr_2N$	29.3	5.0
Cr-N 3	$CrN_{0.49}$	Cr_2N	32.6	4.5
Cr-N 4	$CrN_{0.98}$	CrN	28.8	4.1
Cr-N 5	$CrN_{0.99}$	CrN	33.6	3.8
Cr-N 6	$CrN_{1.00}$	CrN	37.7	3.8
Ti-B-C	$TiB_{1.2}C_{0.6}$	$TiB_2 + TiC$	70.6	2.7

Table 1: Coatings investigated

Coating hardness was determined from the load vs. displacement data measured using a computer controlled microhardness tester (Fischerscope H100). The abrasion resistance was evaluated using a small-scale abrasive wear test (CSEM CaloWear). There, a steel sphere (DIN 1.2067, diameter,

25.4 mm) is rotating against the coated sample in the presence of an aqueous suspension of abrasive particles. In this work, aqueous suspensions of SiC (average grain size, 4 µm) and diamond (average grain size, 1 µm) have been used. The sphere was rotated against the sample at 150 rpm. Fig. 1 shows an example of a typical wear crater in a coated sample. The diameter of the resulting wear crater was determined as a function of the sliding distance by means of a calibrated optical microscope. The wear crater was measured at intervals corresponding to increments in the sliding distance of about 14 m after removing the sphere. After each measurement, the sphere was relocated to the identical position and the typical total sliding distance was 70 m.

The normal force F_N on the specimen is determined by the weight of the sphere and the lateral position of the drive shaft (7). To optimize test conditions for this work, F_N was varied between 0.18 and 0.45 N, measured by a sensitive load cell.
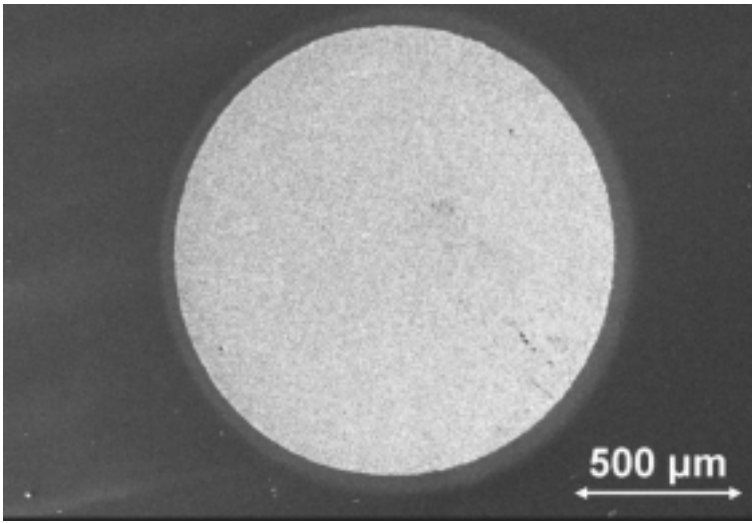

Fig. 1: Scanning electron micrograph of an imposed wear crater in a CrN$_{0.99}$ coating (SiC slurry).

The abrasion wear coefficients of both coating and substrate material is derived from the increasing wear volume depending on sliding distance and normal force during the testing process using the equation described in (7):

$$\frac{s \cdot F_N}{d_a^4} = \left(\frac{K_s - K_c}{K_s \cdot K_c} \right) \cdot \left(\frac{\pi \cdot t}{4 \cdot d_a^2} - \frac{\pi \cdot R \cdot t^2}{d_a^4} \right) + \left(\frac{1}{K_s} \right) \cdot \left(\frac{\pi}{64 \cdot R} \right) \tag{1}$$

There, s is the distance slid by the sphere, d_a is the external diameter of the wear crater, K_s and K_c are the abrasion wear coefficients of substrate and coating, respectively, t is the coating thickness and R is the radius of the sphere. A plot of $(s \cdot F_N/d_a^4)$ against $((\pi \cdot t/4 \cdot d_a^2)-(\pi \cdot R \cdot t^2/d_a^4))$ is thus linear with the intercept and gradient determined by the values of K_c and K_s (see Fig. 2). K_s can be determined directly from the intercept, and this value is then used together with the gradient to provide K_c.
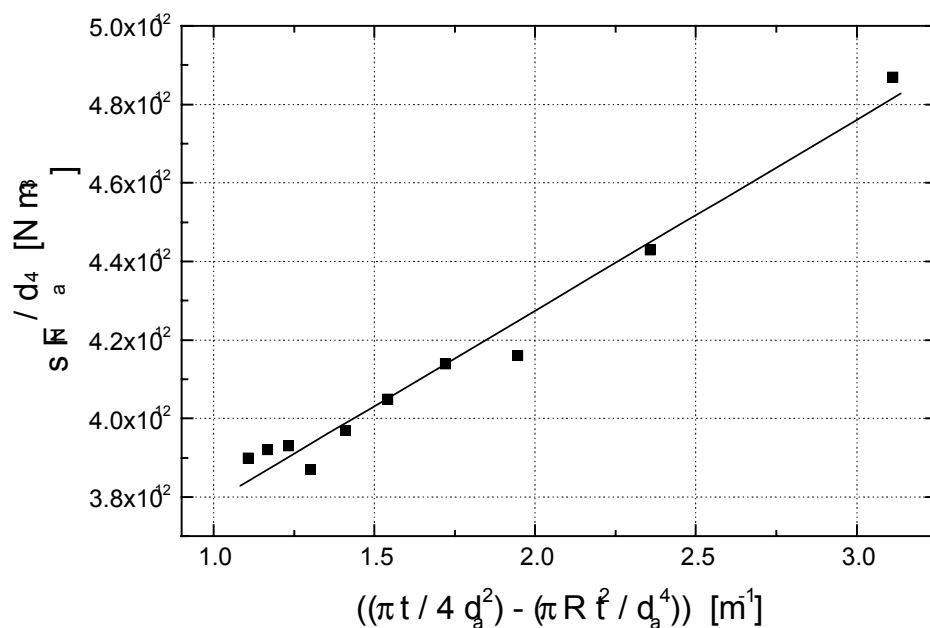
Fig. 2: Plot of abrasion wear data obtained for a $CrN_{1.0}$ coating according to equation (1) using an SiC slurry.

Results and Discussion

The aim of a first test series was to optimize test conditions for the abrasive wear test. Fig. 3 shows the abrasion coefficients determined for a coating of chemical composition $CrN_{1.0}$ deposited onto an austenitic stainless steel substrate as a function of the normal force applied on the sample. The standard deviation of K_c for the loads investigated is well below 5 %. However, to minimize the error in determining K_s, the normal load for all further investigations was adjusted in the range between 0.3 and 0.4 N.
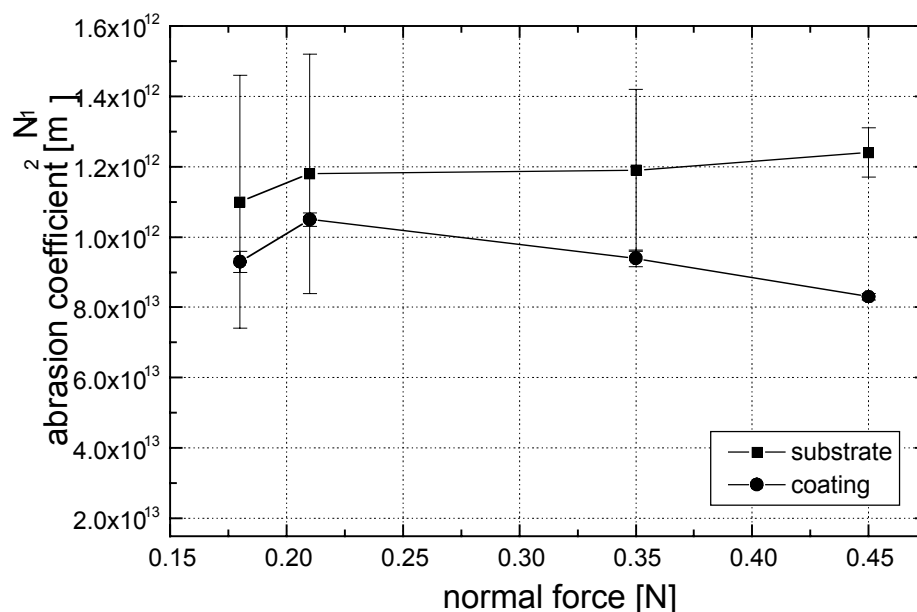

Fig. 3: Dependence of the abrasion coefficients of coating and substrate on the normal force applied for a $CrN_{1.0}$ coating on austenitic stainless steel (SiC slurry).

The abrasion coefficients of Cr-N coatings determined using a SiC abrasive slurry and optimized test parameters is illustrated in Fig. 4 as a function of their chemical composition. There, the phase composition as characterized by X-ray diffraction is also indicated (5). The abrasion coefficient for the Cr coating is about $5.3 \_ 10^{-12}$ m^2 N^{-1}. For the dual-phase coating consisting of a Cr(N) solid solution and Cr$_2$N and for the Cr$_2$N coating, K_c decreases to about $2 \_ 10^{-12}$ m^2 N^{-1}. Coatings close to the composition of stoichiometric CrN yield an abrasion coefficient of about $1 \_ 10^{-12}$ m^2 N^{-1} which is in good agreement to literature values (8).
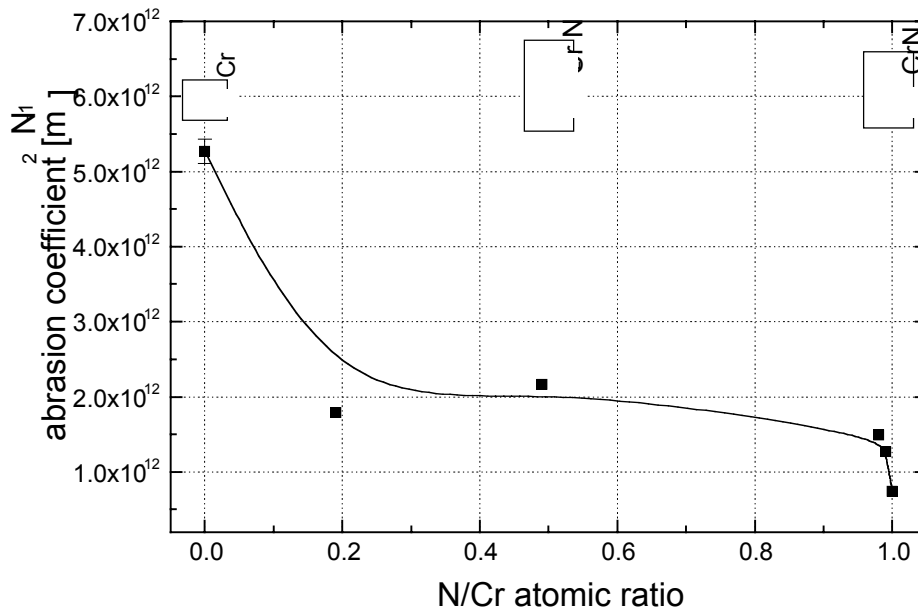
Fig. 4: Dependence of the abrasion coefficients of Cr-N coatings on their chemical and phase compositions (see Table 1, SiC slurry).
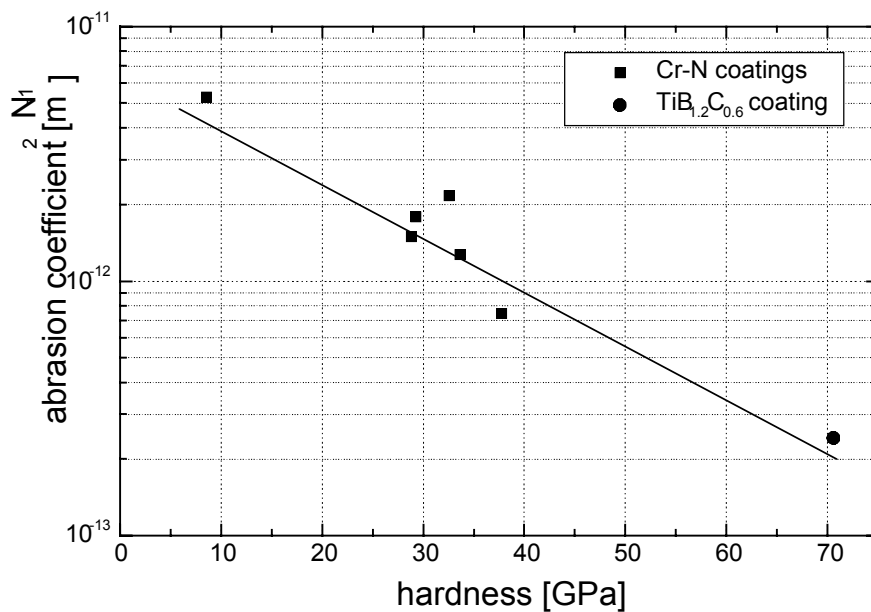
Fig. 5: Correlation between the abrasion coefficients and hardness of Cr-N and Ti-B-C coatings.

Fig. 5 shows the correlation between the abrasion coefficients determined for Cr-N coatings and their hardness. For sake of comparison, the abrasion coefficient determined for a nanocomposite coating of composition $TiB_{1.2}C_{0.6}$ consisting of nanograined TiB_2 and TiC phases (6,9) is also shown. It should be noted that - obviously as a result of the high hardness of this coating of about 70 GPa – application of the SiC slurry in the micro-abrasion test did not yield high-quality wear craters and, consequently, large deviations of the crater dimensions and thus of the K_c and K_s values have been observed. The data point given in Fig. 5 has been obtained for a diamond slurry, where the standard deviation yields a value of about 4 %. Although the coatings investigated show a wide range of hardness values, Fig. 5 shows an excellent correlation between the coating abrasion coefficient and the hardness.

Conclusions

Within this work, several sputtered coatings ranging from Cr through Cr_2N and dual-phase coatings consisting of the solid solution Cr(N) and Cr_2N to CrN single phase coatings as well as a superhard nanocomposite Ti-B-C coating have been investigated with respect to their abrasion resistance and hardness. The results obtained show an excellent correlation between coating hardness and abrasion resistance. Moreover, the micro-scale abrasion test employed offers a simple and inexpensive method for pre-selecting and ranking of coating materials for abrasive wear situations.

Acknowledgements

References

(1)   M.A. Djouadi, P. Beer, R. Marchal, A. Sokolowska, M. Lambertin, W. Precht, C. Nouveau: Surf. Coat. Technol. 116-119 (1999) 508.

(2)   S.J. Bull, R.I. Davidson, E.H. Fisher, A.R. McCabe, A.M. Jones: Surf. Coat. Technol. 130 (2000) 257.

(3)   R. Gåhlin, M. Larsson, P. Hedenqvist, S. Jacobson, S. Hogmark: Surf. Coat. Technol. 90 (1997) 107.

(4)   P. Losbichler, C. Mitterer: Surf. Coat. Technol. 97 (1997) 568.

(5)   P.H. Mayrhofer, G. Tischler, C. Mitterer: Surf. Coat. Technol., submitted.

(6)   C. Mitterer, P.H. Mayrhofer, M. Beschliesser, P. Losbichler, P. Warbichler, F. Hofer, P.N. Gibson, W. Gissler, H. Hruby, J. Musil, J. Vl_ek: Surf. Coat. Technol. 120-121 (1999) 405.

(7)   K.L. Rutherford, I.M. Hutchings: Surf. Coat. Technol. 79 (1996) 231.

(8)   K.L. Rutherford, S.J. Bull, E.D. Doyle, I.M. Hutchings: Surf. Coat. Technol. 80 (1996) 176.

(9)   P.H. Mayrhofer, C. Mitterer: Surf. Coat. Technol., in press.